Volume 1 | Number 1 | Jan 2013 | Pages 1–100

Journal of
Materials Chemistry B

Materials for biology and medicine
www.rsc.org/materialsB

ROYAL SOCIETY
OF CHEMISTRY

ROYAL SOCIETY
OF CHEMISTRY

www.rsc.org/materialsB

Journal Name

Dynamic Article Links ▶

ARTICLE TYPE

Cross-Linking Graphene Oxide-Polyethyleneimine Hybrid Film containing Ciprofloxacin: One-Step Preparation, Controlled Drug Release and Antibacterial Performance

5 **Tiefan Huang,** [a] **Lin Zhang,**[*a] **Huanlin Chen**[a] **and Congjie Gao**[a,b]

A novel drug delivery system based on a graphene oxide film cross-linked by polyethyleneimine was prepared via one-step preparation technique. Due to cross-linking, the stability of the film was
10 significantly improved compared with bare graphene oxide film and extra drug-loading site was endowed to the film by PEI. The release behavior of ciprofloxacin, as a model drug, was investigated under various pH values in vitro, and the results exhibited slow drug release without an initial burst effect. Release kinetic models were employed to represent the drug release processes, and the release behavior of ciprofloxacin of the resulting crosslinking film was consistent with near zero-order kinetics. In
15 comparison to a graphene oxide-polyethyleneimine hybrid film, the ciprofloxacin loaded hybrid film exhibited a significant antibacterial effect due to the ciprofloxacin release and diffusion from of the film. This study provides insight into the design of suitable cross-linking GO hybrid films for biomedical area and many other applications.

Introduction

20   The development of new and effective drug delivery systems with the ability to improve the therapeutic profile and efficacy of therapeutic agents is an important challenge faced by modern medicine.[1, 2] The recent discovery of graphene has been
25 accompanied by increasing investigation of this new material for drug delivery systems.[3] In particular, graphene oxide (GO), which is one of the most important derivatives of graphene, has been widely investigated for application in the biomedical area including for pathogen detection, gene transfection, intracellular
30 monitoring and drug delivery due to its simple preparation procedure and easy processing property.[4-9] The advantages of utilizing GO as an effective carrier for drug delivery include its high aspect ratio, abundant surface chemistry and good dispersion in aqueous solution, which facilitates drug loading in water. For
35 example, for the first time, Dai et al. employed PEGylated nanographene oxide as a nanocarrier to load anticancer drugs via noncovalent physisorption and studied its cellular uptake.[10] Zhang et al. loaded two anticancer drugs on functional graphene oxide to develop a multi-drug delivery system, which can be
40 expanded for use in biomedicine.[11]

However, the cytotoxicity of free GO particles is still controversial. Recent studies indicate that a large dose of GO can cause adverse oxidative stress in the cell and induce a slight loss of cell viability,[12, 13] which would be a potential risk for
45 graphene-based nanoparticles as drug carriers in clinic applications. Therefore, it is much safer to load drugs on graphene in a bulk assembly instead of on an individual graphene nanosheet.

One of the important characteristics for graphene-based
50 nanoparticles is their excellent film formation ability. Graphene-based film is relatively easy to prepare by a facile filtration-assisted assembly method.[14, 15] Several groups have reported preparation of graphene-based films and studied their application in separation.[16-18] For example, Geim et al. constructed a
55 micrometer thick GO membrane that was completely impermeable to liquids, vapors, and gases (even helium) and only allowed unimpeded evaporation of water.[19] The GO film, which was used in the released of drug, has also been discussed occasionally.[20, 21]

60 Although the bare GO film is rather tough in a dry state due to the strong van der Waals interactions and hydrogen bonds between the faces of each sheet,[14] once immersed in water, the film becomes very unstable and tends to disintegrate and re-disperse rapidly because the hydrophilic groups, such as carboxyl, epoxide,
65 carbonyl and hydroxyl groups, on the GO nanosheets can adsorb water.[22, 23] Therefore, the integrity of the simple stacking GO film would be damaged during application in an aqueous solution, and the GO film becomes graphene-based nanoparticles. This

potential risk makes the simple stacking GO film inappropriate for drug release for clinic use.

The most important prerequisite for the practical application of GO films in biomedicine is the stability. Cross-linking between adjacent GO nanosheets in a film can improve the stability of a GO film. Ruoff et al. first reported a cross-linking GO film using polyallylamine (PAA) and divalent ion, respectively. In comparison to a bare GO film, the modified graphene films exhibited excellent mechanical stiffness and strength.[24, 25] Using layer-by-layer deposition, Mi et al. prepared GO films for water treatment where the adjacent GO nanosheets were cross-linked by 1,3,5-benzenetricarbonyl trichloride.[26] In general, the cross-linkers are linear polymers and small molecules or ions resulting in a short distance between the GO nanosheets in the GO cross-linking film. Therefore, the drug-loading capability of the cross-linking film could be low, which is not favorable for graphene film for drug release. Therefore, to choose a proper cross-linker is the key to prepare an ideal GO film for drug delivery.

Polyethyleneimine (PEI) is a hyperbranched polymer, which has been widely studied in many areas, such as biomedicine and membrane separation.[27-29] With the presence of primary, secondary, and tertiary amines, PEI could potentially interact with GO by electrostatic force. In addition, amine groups can easily react with the oxygen functional groups of the GO nanosheets, which cross-links GO nanosheets with covalent bonds.[24, 30, 31] Unlike linear polymers or small molecules or ions, we hypothesized that PEI can expand the distance between the GO nanosheets due to its hyperbranched structure. Another advantage of using a hyperbranched polymer is that drugs can also be loaded into the internal cavities of PEI, which is beneficial for achieving a larger drug-loading amount.[32-34]

In this work, a novel drug delivery system based on a graphene oxide-polyethyleneimine hybrid (GPH) film, in which the graphene oxide nanosheets were cross-linked using PEI, was prepared via a one-step synthesis. Due to cross-linking, the mechanic stability of the film in water environment was significantly improved compared to the bare GO film. Ciprofloxacin (CF), which is a broad-spectrum antimicrobial agent that is widely used in clinical practice, was employed as the model drug to investigate the release behavior of the system. This system exhibited near zero-order kinetic release without an initial burst effect. In comparison to the GO and GPH films, the CF-loaded GPH film exhibited a significant antibacterial effect. The design principles open the door to designing suitable crossing-linking GO hybrid films for application in the biomedical area and many other areas.

Experiments section

Materials

GO was purchased from the XFNANO Material Tech Co. (Nanjing, China). Branched polyethyleneimine (PEI) with a molecular weight of 10 000 was purchased from Sigma-Aldrich (St. Louis, USA). Analytical reagent grade ciprofloxacin hydrochloride (CF, $C_{17}H_{18}FN_3O_3 \cdot HCl$, 367.81g/mol) was obtained from Aladdin Industrial Inc. (Shanghai, China) and used as received. All of the other chemicals were purchased from Sinopharm Chemical Reagent Co. (Shanghai, China). Deionized water (electrical resistivity>17 MΩ·cm) that was used throughout the experimental process was produced in this laboratory. The strains employed in this work was Escherichia coli (E. coli, ATCC 8739).

Preparation of the drug-loaded GPH film

The drug-loaded GPH film was prepared using a one-step procedure. GO powder (10mg) was dispersed in water (100ml) and ultrasonicated for 3 h. The GO dispersion was added to a certain amount of PEI and ultrasonicated to produce the homogeneous GO-PEI hybrid solution. After adding CF (0.1g) to this solution, the mixture was vigorously stirred for 30 min followed by ultrasonication to produce the drug-loaded GO-PEI hybrid solution. The final drug-loaded GPH film was obtained by filtration of the resulting colloid through an acetylcellulose membrane filter (47 mm in diameter, 0.2 μm in pore size). After filtration, the as-prepared film was further under suction for 12 h. The GO and GPH films were also prepared as controls.

Characterization

The SEM images were obtained using field-emission scanning electron microscopy (FE-SEM) Ultra 55 (CorlzeisD Co., Germany) after gold coating. For cross-sectional observation, the film (along with substrate) was immersed in liquid nitrogen and fractured using tweezers and affixed vertically to the stub. Fourier transform infrared (FTIR) spectra were recorded on Bruker Tensor27 spectrometer. The samples were prepared as KBr pellets, and the spectra were calculated from a total of 32 scans. X-ray photoelectron spectroscopy (XPS) was carried out on an Axis-Ultra DLD spectrometer (Kratos Co, USA) using Al Kα radiation at a base pressure of 3×10^{-9} mbar, and the binding energies were referenced to the C1s line at 285 eV from adventitious carbon. A survey scan spectrum was recorded, and the surface elemental composition was calculated from the peak area with a correction for atomic sensitivity. The error in all of the binding energy (BE) values is ±0.1 eV. X-ray diffraction (XRD) was carried out using a X'Pert PRO (PANalytical, Netherland) X-ray diffractometer with Cu KR radiation (λ = 1.5406 Å).

Mechanic stability studies

For quantitative study of mechanical stability of GPH film in water, GO and GPH film with diameter of 4cm was placed in 200 ml of water in a baker, respectively, with constant oscillation. At regular time intervals, the oscillation suspension was withdrawn to test the GO nanosheets concentration using an UV−visible spectrophotometer at 600nm. The tests were performed in triplicate, and the results were recorded as an average with an error bar that represents one standard deviation.

In vitro drug release studies

For the in vitro release studies of CF from the drug-loaded film, a piece of film that was 1 cm×1 cm was placed in 50 ml of water in a test tube with constant shaking at 37 ˚C. At regular time intervals, the release medium was withdrawn from the test tube

and replaced with an equal quantity of water to maintain a constant volume. The accumulated amount of CF released into the medium was measured periodically using an UV−visible spectrophotometer Gold Spectrumlab 54 (Shanghai the Lengguang Technology Co. Ltd., China) at a wavelength of 267 nm. The tests were performed in triplicate, and the results were recorded as an average with an error bar that represents one standard deviation. Cumulative CF release (%) was calculated as follows: $(M_t/M_0) \times 100\%$, where M_t is the amount of CF released from the GPH film at time t and M_0 is the amount of CF initially loaded onto the GPH film.

Antibacterial activity test

Antibacterial activities of the samples were investigated against the growth of E. coli using an inhibition zone test and oscillation release method. Inhibition zone method: All of the samples and utensils were sterilized by autoclaving at 121 ˚C for 20 min prior to each microbiological experiment. The bacterium were cultured in Luria Bertani medium (LB) at 37 ℃ for 12 h on a rotary shaker at 150 rpm. Then, a portion of this bacterium suspension was diluted to a concentration of ~10^5 cells/ml using a gradient method. The CF-loaded GPH film samples (i.e., 1 cm²) was placed on LB agar medium in Petri dishes that had been seeded with 0.2 ml of a ~10^5 cells/ml bacteria suspension. For comparison, GPH film was also used. The plates were examined to determine the zone of inhibition after incubation for 24 h at 37 °C. The area that surrounded the film where the bacteria were not capable of growing was reported as the zone of inhibition. Oscillation release method: the CF-loaded GPH film sample with diameter of 4cm was immersed in LB medium. After oscillation overnight at 37 ℃, the film was removed from the LB medium, and bacterium were cultured in this Luria Bertani medium (LB) at 37 ℃ for 12 h on a rotary shaker at 150 rpm. Then, a portion of this bacterium suspension was diluted and seeded on LB agar medium. For comparison, GPH film was also used. The plates were examined to determine the bacterium colony after incubation of 24h at 37 ℃.

Results and discussions

Preparation and characterization of CF-loaded GPH film.

The strategy for the one-step preparation of CF-loaded GPH films is shown in Figure 1a. First, PEI was added to a GO dispersion to form a uniform mixture. PEI was grafted onto the GO nanosheets via covalent bonds and electrostatic interactions. Then, CF was added to the dispersion. As discussed above, CF was loaded on the GO nanosheet surface and internal cavities of PEI. Finally, the mixture was filtered to obtain the CF-loaded GPH film. Similar to the GO and GPH films, the drug-loaded GPH film exhibited excellent flexibility and return to its original shape without cracks after being rolled up, as shown in Figure 1b.

Due to PEI cross-linking, it is difficult for GO nanosheets to exfoliate from the film into water. Figure 1c shows the bare GO, GPH and CF-loaded GPH films after oscillation (120 rpm) for 6 h in PBS buffer. The GO film is mechanically unstable in a water environment. During the oscillation process, the GO nanosheets gradually detached from the film, which resulted in the water in the petri dish becoming yellow brown in color. In parallel, the water in the petri dish of the GPH and CF-loaded GPH films after

the same oscillation period remained clear and clean, which indicated that the GO film stability significantly improved due to PEI cross-linking. To study the mechanic stability of films in water environment, GO nanosheets concentration in oscillation solution of films with time was measured. As shown in Figure 2, for GO film, GO nanosheets concentration in oscillation suspension increased rapidly. While, for GPH, nearly no GO nanosheets were detected in oscillation suspension. Further, we employed a classic colony counting method to measure the microbial viability of E. coli treated with a PBS buffer containing the GO and GPH films after oscillation. The PBS buffer containing the GO film nearly suppressed the growth of E. coli, which is in contrast to the results from the PBS buffer containing the GPH film (see ESI, Figure S1).
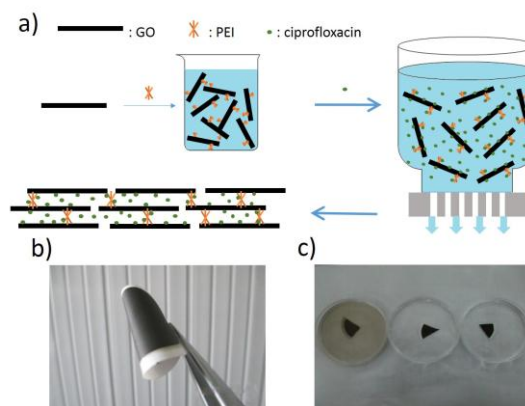

Figure 1. a) Schematic illustration of the formation of a drug-loaded GPH film via vacuum filtration process. b) Bent CF-loaded GPH film. c) Photographic images of the GO film, GPH film and CF-loaded GPH film (from left to right) after oscillation (120 rpm) for 6 h in a PBS buffer.
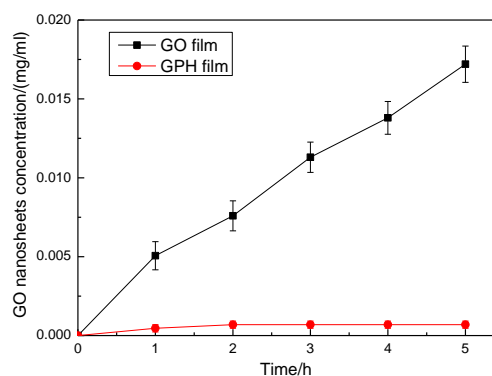

Figure 2. GO nanosheets concentration profiles of films oscillated in water environment with time.

The successful modification of GO with PEI and loading of the drug into the film were confirmed by Fourier transform infrared (FTIR) spectroscopy and X-ray photoelectron spectroscopy (XPS) (Figure 3). After modifying the graphene oxide sheets with PEI, an increase in the peak intensity at 1462 cm⁻¹, which corresponds to stretching of the new C-N bonds and residual group of PEI, was observed in the FTIR spectrum of the GPH film (curve b,

Figure 3a).[30, 35] In comparison to GO film, the peak intensity of GPH film at 2923 cm^{-1} and 2852 cm^{-1}, which correspond to C-H stretching vibrations of PEI, substantially increased. The peak in the region corresponding to -COOH stretching vibration at 1738 cm^{-1} decreased, which indicated also electrostatic interaction between GO and PEI. In addition, a peak appeared at 1585 cm^{-1}, which corresponds to the unoxidized aromatic domain of graphene oxide.[36] This result demonstrates that, as with other organic amines, PEI modified GO via the amine-epoxy reaction and electrostatic interactions and reduce GO to some extent, which would facilitate the loading of other molecules onto the GO nanosheets via π-π stacking.[37, 38] Due to CF loading, the FTIR spectrum of the CF-loaded CPH film (curve d, Figure 3a) consists of the combined spectral band features of the CF and GPH films.

Figure 3b shows the wide scan spectra of GO film, the GPH film and the drug-loaded GPH film; the elements component percentage of GO film and GPH film are displayed in Table S1. In contrast to GO, a peak at 396.6 eV corresponding to the N1s binding energy was observed for the GPH film. For the CF-loaded GPH film, another peak was observed at approximately 684.8 eV and is evidence of the existence of the F element in CF. Higher resolution data of the C1s peak for GO film and GPH film are shown in Figures 3c and d, respectively. Although the C1s regions of the spectrum for the GPH film (Figure 3d) also contains the same oxygen-containing functional groups, some of their peak intensities are much smaller than those in GO, which indicated that GO has been partially reduced by PEI. In addition, there is an additional predominant peak component at approximately 286 eV, which is due to the C–N peak. For clear comparison, the percentages of each carbon component (exclude C-N) calculated from the peak area for GO film and GPH film are listed in Table S1. After PEI grafting, the change in the C-OH and C-O-C peak intensities indicate the opposite trend. These observations clearly suggest that PEI grafts onto the GO via the amine-epoxy reaction.[39] According to the XPS results and the filtrate collected, the CF loading capacity of the GPH film was as high as 1.71 mg/mg (see ESI). This result demonstrated the excellent drug-loading capability of the GPH film.
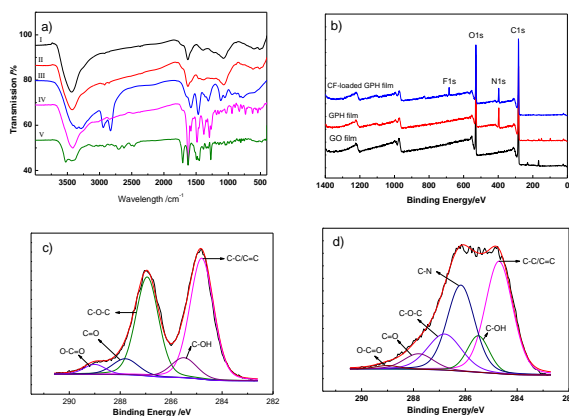

Figure 3. a) FTIR spectra of GO film (a), GPH film (b), PEI (c), CF-loaded GPH film (d) and CF (e). b) Survey XPS spectra and c-d) C1s XPS spectra of the GO and GPH films.

The X-ray diffraction (XRD) patterns of the GO film, GPH film and CF-loaded GPH film after drying as well as the CF powder was displayed in Figure 4a. XRD pattern of GO film shows a single sharp diffraction peak at 2θ = 11.5°. In the GPH film curve, a new peak appeared at 2θ = 6.0°, and the peak at 2θ = 11.5° has a much weaker intensity and larger FWHM than that of GO film (Figure 4a (inset)). These results imply that the PEI chains were sandwiched between the GO sheets.[40] Due to the expected functional groups that are present on the GO nanosheets and PEI, we hypothesize that two modes of interactions for PEI with the GO nanosheets are present in the GPH film as follows: (1) bridging the edges of the sheets through electrostatic interactions between the carboxyl groups of GO and the amino groups of PEI and (2) intercalating between the GO nanosheets via chemical bonds formed between the epoxy groups of the GO and the primary amine groups of PEI. For the CF-loaded GPH film, the peak at 6.0 ° disappeared, which was due to the growth of a drug crystal that disrupted the well laminar structure of the GPH film after drying. The XRD pattern of the CF-loaded GPH film shows the different characteristics of CF, which include strong interactions between CF and the GPH film and are consistent with the FTIR results. In order to study the structure and morphology of films, SEM characterization was carried out. As shown in Figure 4b and c, both GO and the GPH film exhibited well-stacked structures. Due to PEI intercalation, the GPH film becomes thicker and looser compared to the GO film. The CF-loaded GPH film also exhibited a lamellar structure (Figure 4d), but to some extent, the structure was disrupted by the growth of drug crystals after film drying. It is important to note that a large quantity of drug was stored in this lamellar structure, which indicated the excellent ability of the GPH film to act as a drug reserve.
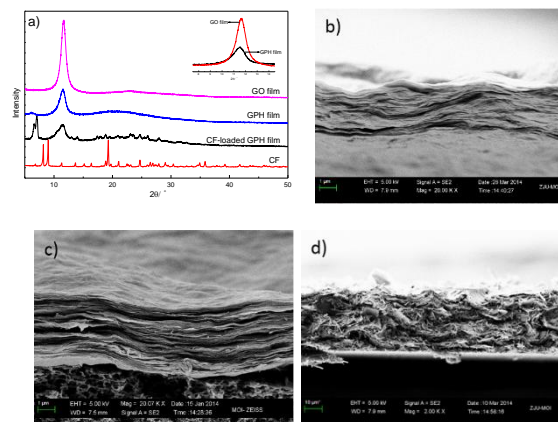

Figure 4. a) XRD patterns. SEM images of b) cross-section of GO film, c) GPH film and d) CF-loaded GPH film.

In vitro drug release behaviour

The release behavior of CF from the GPH film was investigated in a PBS buffer with different pH values, as shown in Figure 5. Each point with an error bar represents one standard deviation for three measurements. At physiological pH (i.e., 7.4), CF releases slowly from the GPH film, and all of the CF was released from the GPH film in as long as 42 h. However, at a pH of 5.5, the CF release rate was higher. For comparison, approximately 62% and 24% of the loaded CF was released after 9 h at a pH of 5.5 and 7.4 respectively. The accelerated drug release under acid conditions may be due to weakened electrostatic interactions

between CF and PEI. At a pH of 5.5, both CF and PEI would be positively ionized resulting in an electrostatic repulsive force between them. In addition, as the pH of the release medium became more acid, ionization of the amine groups in the PEI structure increased, which resulted in an electrostatic repulsive interaction between the PEI chains. Therefore, PEI would exhibit a more stretched molecular structure that would further enlarge the interplanar distance between the GO nanosheets resulting in decreased diffusion resistance for drug release-out. Based on the discussion above, the role of PEI in this work is as follows: (1) partial reduction of GO, which facilitates π-π interactions between CF and GO resulting in a higher drug loading; (2) acts as a cross-linker to improve the mechanic stability of the film; (3) acts as an extra drug-loading site to enhance the drug-loading capability of the film; and (4) acts as a pH-response site for controlling drug release. This pH-dependent release profile was also observed other systems such as GO nanosheets,[8, 9] PEGylated GO nanosheets[41] and Pluronic F127-GO nanosheets.[42] In addition to the release rate difference, the cumulative release amount of CF from the film under various pH values was also different. Under acid conditions, the CF release amount was approximately 73%, which is slightly less than that in a neutral release medium (i.e., 81%). The less cumulative release amount at a pH of 5.5 may be due to increased hydrogen bonding between the –COOH group in CF and the –OH group on GO. This increased interaction between CF and the GO nanosheets results in more CF being retained on the GO nanosheets of the film instead of being released.

It is important to note that the release profile did not exhibit an initial rapid release phase (burst effect), which has been commonly observed in many other drug delivery systems.[43, 44] Because the drug loading was more than 50% of the total GPH film mass, it is rather interesting to observe no burst release phenomenon, which may be due to most of the drug being captured and distributed in the lamellar structure of the film rather than the surface, which as confirmed by SEM and discussed above. In addition, the GO and PEI associated with the CF by electrostatic interactions, hydrogen bonds and π-π interactions, which increased the affinity for this drug resulting in a constant release from the film without displaying a burst effect.
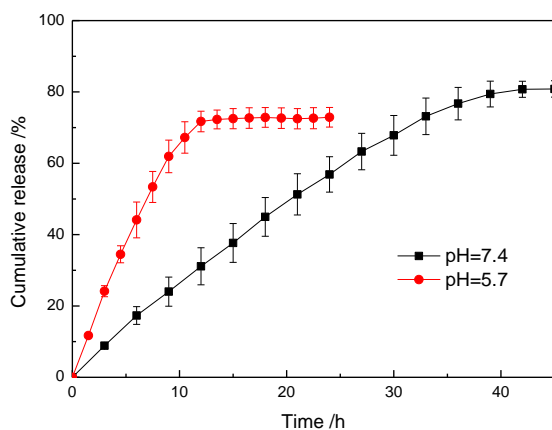
one standard deviation).

We also studied the in vitro release kinetics (or pharmacokinetics) of CF from the GPH film by fitting the drug release data to a suitable model. Five of the most applied mathematical models were employed to study the release of CF from the GPH film.[45-48] The zero-order model (Equation (1)), first-order model (Equation (2)), Higuchi model (Equation (3)), Bhaskar model (Equation (4)) and Ritger-Peppas model (Equation (5)) are shown below,

$$\frac{M_t}{M_\infty} = \mathrm{k}t \qquad (1)$$

$$\log\left(1 - \frac{M_t}{M_\infty}\right) = -(\mathrm{k}/2.303) \quad (2)$$

$$\frac{M_t}{M_\infty} = \mathrm{k}t^{0.5} \qquad (3)$$

$$\log\left(1 - \frac{M_t}{M_\infty}\right) = -kt^{0.65} \quad (4)$$

$$\frac{M_t}{M_\infty} = kt^n \qquad (5)$$

where M_t is the amount of drug released at time t, M_∞ is the total amount of drug released, k is the release kinetic constant and n is the diffusional exponent that provides an indication of the mechanism of drug release. For a thin hydrogel film, when n=0.5, the drug release mechanism follows Fickian diffusion. When n=1, Case II transport occurs, leading to zero-order release. When the value of n is between 0.5 and 1, anomalous transport was observed. The model with the highest correlation coefficients (R^2) between the observed and the fitted data was selected as the one with the best fit. As indicated in Table 2, CF release from the GPH film exhibited a better fit with the Ritger-Peppas model compared to the zero-order model, first-order model, Higuchi model and Bhaskar model. Both n values at the two different pH values were larger than 0.89, which suggested that Case II transport dominates the release of CF from the GPH film. Therefore, the release is near zero-order kinetic.

Table 1. Correlation coefficients R^2 for CF-loaded GPH film systems at 37 °C under different pH after fitting the release profile obtained using different release models.

Release at different pH	Zero-order Model R^2	First-order Model R^2	Higuchi Model R^2	Bhaskar Model R^2	Ritger-Peppas Model	
					n	R^2
pH=5.7	0.9712	0.8068	0.9330	0.6597	n=0.9593	0.9975
pH=7.4	0.9839	0.9023	0.9159	0.7609	n=0.8951	0.9993

Determination of antibacterial activity

The antibacterial activity of the CF-loaded GPH film was examined against Gram-negative E. coli. The inhibition zone

Figure 5. In vitro release profiles of CF-loaded GPH hybrid films in a PBS buffer with different pH values (the error bars represent

method is a simple but effective antibacterial test method for evaluating the antibacterial properties. Figure 6 shows the antimicrobial test results for the GPH film and CF-loaded GPH film. The CF-loaded GPH film exhibited distinctive antibacterial

5 effects against E. coli with a clear zone of diameter of 4 cm forming around the film. However, no inhibition zone was formed around GPH film sample These results suggested that the GPH films cannot inhibit E. coli, while, CF-loaded GPH film can effectively inhibit E. coli growth and reproduction because CF

10 release from and diffuse out,. In order to further prove it, we tested the antibacterial activity by oscillation release method. As shown in Figure 6c and d, no colony was existed on the plate seed by CF-loaded GPH film oscillation LB medium, while on the plate seed by GPH film oscillation LB medium, bacterium colony

15 existed obviously. Therefore, the CF-loaded GPH film, which exhibits good antibacterial properties, can be applied as an excellent delivery system for storing antibacterial drugs, maintaining antibacterial activity, and achieving controlled release of antibacterial drugs.
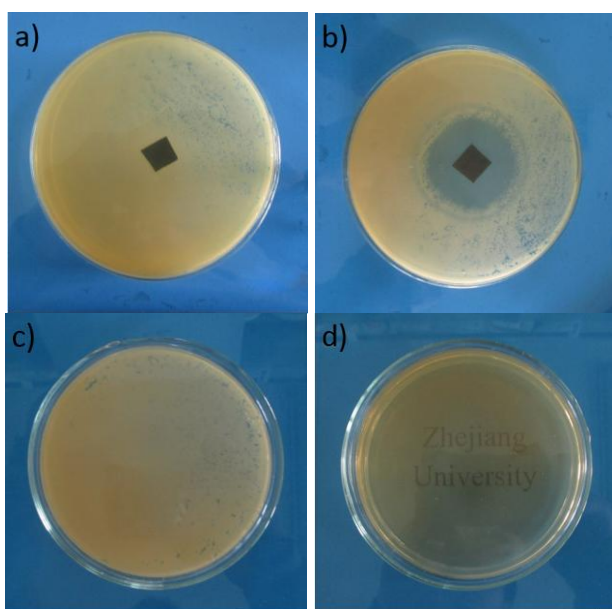
20

Figure 6. Antibacterial activity determination. Inhibition zone tests of a) GPH film and b) CF-loaded GPH film against E. coli
25 on LB agar medium. Oscillation release test of c) GPH film and d) CF-loaded GPH film oscillation LB medium seeded on LB agar medium

Conclusions

30 In this study, we have demonstrated a novel cross-linking GO film loaded with CF for controlled release. The film was prepared using a simple one-step method. The merit of this method lies in its low cost, use of nontoxic agents and easy applicability, which is especially favorable for scale-up in industry. Using various
35 characterization techniques, GO was successfully cross-linked by PEI. Due to cross-linking, the mechanic stability of the film significantly improved compared to uncross-linked GO film, which effectively prevented the GO nanosheets exfoliating from the film during practical application resulting in low risk of

40 cytotoxicity. Under various pH values, the film exhibited low drug release without an initial burst effect, which demonstrates its potential use as an interesting drug carrier. In the release kinetics study, the release of CF from the film followed near zero-order kinetics. In addition, because CF can be released and diffused out
45 of the film, the CF-loaded GPH film exhibited good antibacterial activity. Our approach is the first utilization of a cross-linked GO film as a drug carrier, and this result opens the door for designing suitable cross-linked GO hybrid films for application in the biomedical area and many other areas.

Notes and references

a Key Laboratory of Biomass Chemical Engineering of MOE, Department of Chemical and Biological Engineering, Zhejiang
60 *University, Hangzhou 310027, China. Fax: (+)86-571-87952121; Tel: (+)86-571-87953802; E-mail: linzhang@zju.edu.cn*

b College of Chemistry and Chemical Engineering, Ocean University of China 266100, China.

65 † Electronic Supplementary Information (ESI) available: bacteria viability test of E. coli with oscillation suspensions of the GO and GPH films, CF loading capacity of GPH film, calibration curve of CF and GO nanosheets, relative atomic mass concentrations in the GO film and GPH film. See DOI: 10.1039/b000000x/

70

1.   Y. Zhang, H. F. Chan and K. W. Leong, *Advanced Drug Delivery Reviews*, 2013, 65, 104-120.
2.   P. Couvreur, *Advanced Drug Delivery Reviews*, 2013, 65, 21-
75   23.
3.   S. Goenka, V. Sant and S. Sant, *J. Control. Release*, 2014, 173, 75-88.
4.   J. H. Jung, D. S. Cheon, F. Liu, K. B. Lee and T. S. Seo, *Angewandte Chemie-International Edition*, 2010, 49, 5708-
80   5711.
5.   L. Feng, S. Zhang and Z. Liu, *Nanoscale*, 2011, 3, 1252-1257.
6.   H. Q. Dong, Y. Y. Li, J. H. Yu, Y. Y. Song, X. J. Cai, J. Q. Liu, J. M. Zhang, R. C. Ewing and D. L. Shi, *Small*, 2013, 9, 446-456.
85 7.   M. L. Chen, Y. J. He, X. W. Chen and J. H. Wang, *Bioconjugate Chem.*, 2013, 24, 387-397.
8.   H. Pandey, V. Parashar, R. Parashar, R. Prakash, P. W. Ramteke and A. C. Pandey, *Nanoscale*, 2011, 3, 4104-4108.
9.   R. Jin, X. J. Ji, Y. X. Yang, H. F. Wang and A. N. Cao, *Acs*
90   *Applied Materials & Interfaces*, 2013, 5, 7181-7189.
10.   Z. Liu, J. T. Robinson, X. M. Sun and H. J. Dai, *Journal of the American Chemical Society*, 2008, 130, 10876-+.
11.   L. M. Zhang, J. G. Xia, Q. H. Zhao, L. W. Liu and Z. J. Zhang, *Small*, 2010, 6, 537-544.
95 12.   Y. L. Chang, S. T. Yang, J. H. Liu, E. Dong, Y. W. Wang, A. N. Cao, Y. F. Liu and H. F. Wang, *Toxicol. Lett.*, 2011, 200, 201-210.
13.   J. H. Liu, S. T. Yang, H. F. Wang, Y. L. Chang, A. N. Cao and Y. F. Liu, *Nanomedicine*, 2012, 7, 1801-1812.
100 14.   D. A. Dikin, S. Stankovich, E. J. Zimney, R. D. Piner, G. H. B. Dommett, G. Evmenenko, S. T. Nguyen and R. S. Ruoff, *Nature*, 2007, 448, 457-460.

15. X. W. Yang, J. W. Zhu, L. Qiu and D. Li, *Advanced Materials*, 2011, 23, 2833-+.

16. H. B. Huang, Y. Y. Mao, Y. L. Ying, Y. Liu, L. W. Sun and X. S. Peng, *Chem. Commun.*, 2013, 49, 5963-5965.

17. H. Li, Z. N. Song, X. J. Zhang, Y. Huang, S. G. Li, Y. T. Mao, H. J. Ploehn, Y. Bao and M. Yu, *Science*, 2013, 342, 95-98.

18. Y. Han, Z. Xu and C. Gao, *Advanced Functional Materials*, 2013, 23, 3693-3700.

19. R. R. Nair, H. A. Wu, P. N. Jayaram, I. V. Grigorieva and A. K. Geim, *Science*, 2012, 335, 442-444.

20. B. Yuan, T. Zhu, Z. X. Zhang, Z. Y. Jiang and Y. Q. Ma, *J. Mater. Chem.*, 2011, 21, 3471-3476.

21. Y. Wang, D. Zhang, Q. Bao, J. Wu and Y. Wan, *J. Mater. Chem.*, 2012, 22, 23106-23113.

22. D. R. Dreyer, S. Park, C. W. Bielawski and R. S. Ruoff, *Chemical Society Reviews*, 2010, 39, 228-240.

23. N. V. Medhekar, A. Ramasubramaniam, R. S. Ruoff and V. B. Shenoy, *ACS Nano*, 2010, 4, 2300-2306.

24. S. Park, D. A. Dikin, S. T. Nguyen and R. S. Ruoff, *Journal of Physical Chemistry C*, 2009, 113, 15801-15804.

25. S. Park, K. S. Lee, G. Bozoklu, W. Cai, S. T. Nguyen and R. S. Ruoff, *ACS Nano*, 2008, 2, 572-578.

26. M. Hu and B. X. Mi, *Environmental Science & Technology*, 2013, 47, 3715-3723.

27. S. P. Sun, T. A. Hatton and T. S. Chung, *Environmental Science & Technology*, 2011, 45, 4003-4009.

28. M. S. Abd Rahaman, L. Zhang, L. H. Cheng, X. H. Xu and H. L. Chen, *Rsc Advances*, 2012, 2, 9165-9172.

29. E. Andreoli, R. Suzuki, A. W. Orbaek, M. S. Bhutani, R. H. Hauge, W. Adams, J. B. Fleming and A. R. Barron, *Journal of Materials Chemistry B*, 2014, 2, 4740-4747.

30. V. H. Luan, H. N. Tien, L. T. Hoa, T. M. H. Nguyen, E. S. Oh, J. Chung, E. J. Kim, W. M. Choi, B. S. Kong and S. H. Hur, *Journal of Materials Chemistry A*, 2013, 1, 208-211.

31. W. S. Hung, C. H. Tsou, M. De Guzman, Q. F. An, Y. L. Liu, Y. M. Zhang, C. C. Hu, K. R. Lee and J. Y. Lai, *Chemistry of Materials*, 2014, 26, 2983-2990.

32. Y. F. Zhou, W. Huang, J. Y. Liu, X. Y. Zhu and D. Y. Yan, *Advanced Materials*, 2010, 22, 4567-4590.

33. X. F. Hu and J. Ji, *Biomacromolecules*, 2011, 12, 4264-4271.

34. Y. Liu, Y. Fan, X. Y. Liu, S. Z. Jiang, Y. Yuan, Y. Chen, F. Cheng and S. C. Jiang, *Soft Matter*, 2012, 8, 8361-8369.

35. S. Bose, T. Kuila, M. E. Uddin, N. H. Kim, A. K. T. Lau and J. H. Lee, *Polymer*, 2010, 51, 5921-5928.

36. T. Szabo, O. Berkesi, P. Forgo, K. Josepovits, Y. Sanakis, D. Petridis and I. Dekany, *Chemistry of Materials*, 2006, 18, 2740-2749.

37. N. H. Kim, T. Kuila and J. H. Lee, *Journal of Materials Chemistry A*, 2013, 1, 1349-1358.

38. H. L. Ma, H. B. Zhang, Q. H. Hu, W. J. Li, Z. G. Jiang, Z. Z. Yu and A. Dasari, *Acs Applied Materials & Interfaces*, 2012, 4, 1948-1953.

39. J. F. Che, L. Y. Shen and Y. H. Xiao, *J. Mater. Chem.*, 2010, 20, 1722-1727.

40. H. Bai, C. Li, X. L. Wang and G. Q. Shi, *Journal of Physical Chemistry C*, 2011, 115, 5545-5551.

41. X. M. Sun, Z. Liu, K. Welsher, J. T. Robinson, A. Goodwin, S. Zaric and H. J. Dai, *Nano Res.*, 2008, 1, 203-212.

42. H. Q. Hu, J. H. Yu, Y. Y. Li, J. Zhao and H. Q. Dong, *Journal of Biomedical Materials Research Part A*, 2012, 100A, 141-148.

43. T. R. Thatiparti, A. J. Shoffstall and H. A. von Recum, *Biomaterials*, 2010, 31, 2335-2347.

44. T. Y. Wu, Q. C. Zhang, W. P. Ren, X. Yi, Z. B. Zhou, X. C. Peng, X. W. Yu and M. D. Lang, *Journal of Materials Chemistry B*, 2013, 1, 3304-3313.

45. R. W. Korsmeyer, R. Gurny, E. Doelker, P. Buri and N. A. Peppas, *International Journal of Pharmaceutics*, 1983, 15, 25-35.

46. J. M. Chern, W. F. Lee and M. Y. Hsieh, *Industrial & Engineering Chemistry Research*, 2004, 43, 6150-6156.

47. L. Serra, J. Domenech and N. A. Peppas, *Biomaterials*, 2006, 27, 5440-5451.

48. H. Zhang, K. Zou, S. H. Guo and X. Duan, *Journal of Solid State Chemistry*, 2006, 179, 1792-1801.

Table of Contents Graphic
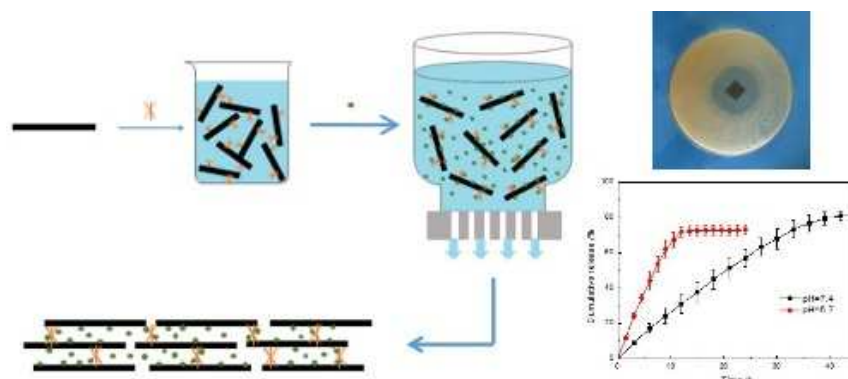
Grapheme oxide film was cross-linked by polyethyleneimine as a novel drug delivery system which showed excellent antibacterial performance.